Cronfa - Swansea University Open Access Repository

_____

This is an author produced version of a paper published in :
Environmental Science & Technology

Cronfa URL for this paper:
http://cronfa.swan.ac.uk/Record/cronfa20015

_____

_____

Enhancing Surface Methane Fluxes from an Oligotrophic Lake: Exploring the Microbubble Hypothesis

Daniel F. McGinnis,*,[†,‡] Georgiy Kirillin,[†] Kam W. Tang,[§] Sabine Flury,[†] Pascal Bodmer,[†] Christof Engelhardt,[†] Peter Casper,[†] and Hans-Peter Grossart[†]

[†]Leibniz-Institute of Freshwater Ecology and Inland Fisheries (IGB), Berlin, Germany
[‡]Institute F.-A. Forel, Section of Earth and Environmental Sciences, Faculty of Sciences, University of Geneva, Geneva, Switzerland
[§]Department of Biosciences and Centre for Sustainable Aquatic Research (CSAR), Swansea University, Swansea, United Kingdom

Ⓢ *Supporting Information*

ABSTRACT: Exchange of the greenhouse gases carbon dioxide (CO_2) and methane (CH_4) across inland water surfaces is an important component of the terrestrial carbon (C) balance. We investigated the fluxes of these two gases across the surface of oligotrophic Lake Stechlin using a floating chamber approach. The normalized gas transfer rate for CH_4 (k_{600,CH_4}) was on average 2.5 times higher than that for CO_2 (k_{600,CO_2}) and consequently higher than Fickian transport. Because of its low solubility relative to CO_2, the enhanced CH_4 flux is possibly explained by the presence of microbubbles in the lake's surface layer. These microbubbles may originate from atmospheric bubble entrainment or gas supersaturation (i.e., O_2) or both. Irrespective of the source, we determined that an average of 145 L m^{-2} d^{-1} of gas is required to exit the surface layer via microbubbles to produce the observed elevated k_{600,CH_4}. As k_{600} values are used to estimate CH_4 pathways in aquatic systems, the presence of microbubbles could alter the resulting CH_4 and perhaps C balances. These microbubbles will also affect the surface fluxes of other sparingly soluble gases in inland waters, including O_2 and N_2.
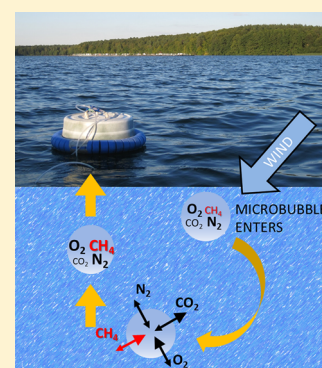
INTRODUCTION

Inland lakes and reservoirs cover ∼3% of the global land surface.[1] These aquatic systems receive and transform substantial amounts of organic carbon (C). Currently, however, they are excluded from the terrestrial greenhouse gas (GHG) balance.[2,3] While it is estimated that inland waters receive 2.9 Pg C y^{-1} from the surrounding landscape, only ∼50% is buried (21%) or transported to the sea (∼31%). Therefore, about half of the allochthonous C is returned to the atmosphere as either carbon dioxide (CO_2) or methane (CH_4) via gas exchange.[4] While methane emissions from inland waters are generally considered small compared to CO_2,[3,5] the climatic forcing on a per mass basis is substantially (∼25×) higher.[6] However, because of the complex flux pathways, and even epilimnetic CH_4 sources,[7,8] there is a large degree of uncertainty in GHG emissions, especially freshwater CH_4 fluxes.[5,9]

Diffusive exchange of CO_2 and CH_4 across the water surface is a key emission pathway that is generally assumed to follow Fickian transport.[9,10] The exchange coefficient, k, is normalized as k_{600} to account for temperature and molecular diffusivity variations among gases, and in a system driven by Fickian diffusion, k_{600} can be used to compare the transport of different gases.[11,12] The k_{600} value is strongly affected by water-side turbulence[13−16] and increases with sea-surface roughness, rain, and wave (both micro- and large-scale) breaking.[17] In lakes and reservoirs, turbulence is often driven by wind; however, as turbulence is difficult to measure, k_{600} estimates are often related to wind speed.[13,18] These wind-parametrizations tend to underestimate diffusive fluxes, as convective mixing due to surface buoyancy loss (cooling) also strongly drives k_{600} values, particularly at low wind speeds.[14,17]

Besides Fickian transport, the presence of surface microbubbles (diameters generally <1 mm[19]) has been proposed to increase the surface fluxes of sparingly soluble gases.[20,21] Not to be confused with sediment methane ebullition, microbubbles are introduced into the surface layer because of, for example, breaking waves, precipitation, or gas-supersaturation (e.g., from primary production).[21] Microbubble entrainment has also been associated with Langmuir circulation,[22] and in lakes, bubble entrainment can occur at wind speeds from 3 to 8 m s^{-1}.[17] Because of their small size, microbubbles both remain in the surface layer for long periods of time (i.e., days)[23] and equilibrate rapidly with other dissolved gases in the water where they are exposed.[20] The microbubble phenomenon, however, has only recently been proposed as an important flux pathway for CH_4 in inland aquatic systems.[9,10] Prairie and del Giorgio[9] report a ∼2.3 fold increase in k_{600,CH_4} versus k_{600,CO_2} measured on several meso- and oligotrophic lakes and a newly impounded reservoir. The authors attribute this enhanced k_{600,CH_4} to the presence of microbubbles. Because CO_2 is much more soluble than CH_4, its flux is expected to be less affected.

We investigate microbubble-enhanced CH_4 fluxes from an oligotrophic lake. The study combines flux measurements using a floating chamber attached to a portable GHG (CH_4 and CO_2) analyzer, together with turbulence measurements. We use a combination of bubble-modeling and a system-analytical approach to investigate the measured fluxes, and we estimate the volume of gas bubble exchange required to produce our observed fluxes. We extrapolate our model results to investigate the role of microbubbles on oxygen fluxes and, finally, we comment on their possible sources and impacts.

■ MATERIALS AND METHODS

Study Site. The 24 h measurement campaign was performed in 2013 (24 August 20:00 to 25 August 21:00) on Lake Stechlin (53°9.69′N, 13°1.89′E; Germany; Figure S1 of the Supporting Information). Measurements were performed in the SW section of the lake (ca. 25−30 m water depth) and are summarized in Table 1. Oligotrophic Lake Stechlin has a maximum depth of 69.5 m and a surface area of 4.3 km².[24,25] Studies of its sediments showed very low methanogenic activities,[26−28] mainly occurring at sediment depths below 20 cm.[29] The resulting porewater CH_4 concentrations are low, and subsequently no sediment-methane ebullition was found.[26]

Floating Chamber and Gas Analyzer. We measured gaseous CO_2 and CH_4 emissions at the water−air interface with a floating chamber attached to a portable GHG analyzer (Los Gatos Research, Inc., USA). The floating chamber consisted of an inverted plastic container with foam elements for floatation (Figure S2 of the Supporting Information). To minimize artificial turbulence effects, the buoyancy element was adjusted so that as little as possible of the chamber penetrated below the water surface (∼2 cm) while still ensuring an effective seal.[16,30] The chamber was painted white to minimize heating. Two gas ports (inflow and outflow) were installed at the top of the chamber and were connected to the GHG analyzer via two 5 m gastight tubes (Tygon 2375). The GHG analyzer measured the gaseous CO_2 and CH_4 concentrations in the chamber every 1 s. Transects were performed with the chamber deployed and kept at a distance of ∼3 m from a small rowboat. The boat and chamber were allowed to freely drift, with the chamber floating in the general direction and speed of the surface water velocity to minimize artificial disturbance. Fluxes were obtained by the slopes of the resolved CH_4 and CO_2 curves over the first ∼8 min (see Figures S3 and S4 of the Supporting Information), when the slopes were approximately linear ($R^2 > 0.98$).

Dissolved Gases. Dissolved pCO_2 and CH_4 sensors (HydroC, CONTROS Systems & Solutions GmbH, Germany) were deployed off the side of the boat at ∼0.5 m depth during the entire campaign, and they recorded data every 10 s. The CH_4 sensor was calibrated with measured CH_4 water samples obtained from the surface water of the lake. The pCO_2 sensor was factory calibrated shortly before the campaign (July 2013) and was corrected for drift postcampaign by CONTROS.[31] A YSI multiprobe (6600 V2; YSI Inc., USA) was deployed alongside the CONTROS sensors, which recorded temperature and dissolved oxygen (O_2) with a 10 s sampling frequency.

CH_4 Sampling and Measurements. Water sample profiles for dissolved CH_4 were collected with a Ruttner water sampler at a fixed location (near the weather station; water depth = 69 m) on four occasions during the campaign (August 24−25, 2013): afternoon (17:00), midnight, before sunrise (05:30), and noon. On board, the water was carefully filled into 120 mL glass bottles and was sealed gastight with butyl rubber septa and

Table 1. Transect-Averaged Atmospheric and Water Column Parameters, Fluxes (F), and Calculated k_{600}[a]

	time	wind 10 m (m s⁻¹)	T_{air} (°C)	rel. hum. (%)	[CH₄]atm (ppm)	[CO₂]atm (ppm)	T_{water} (°C)	$\log_{10}\varepsilon$ (W kg⁻¹)	[CH₄]aq (ppm)	[CO₂]aq (ppm)	F_{CH_4} (mmol m⁻² d⁻¹)	F_{CO_2} (mmol m⁻² d⁻¹)	k_{600} CH₄ (m d⁻¹)	k_{600} CO₂ (m d⁻¹)
1	20:43	5.4	17.8	68.6	1.94	401.5	20.45	−5.24	294.6	222.5	1.29	−13.43	4.1	2.75
2	0:04	3.2	16.3	76.6	1.95	399.5	20.42	−5.19	283.9	230.8	1.43	−14.06	4.8	2.14
3	1:59	4.0	15.6	73.2	1.98	404.0	20.34	−5.33	289.3	233.3	2.42	−26.85	7.9	4.03
4	4:57	3.4	14.3	72.3	1.98	410.9	20.26	−5.24	255.2	234.6	1.88	−23.41	6.9	3.40
5	6:45	3.8	14.9	70.4	1.99	411.0	20.20	−5.21	252.4	237.0	1.01	−13.40	3.7	1.97
6	9:30	4.0	19.6	52.8	2.2	397.2	20.20	−5.02	243.2	236.8	2.00	−20.25	7.7	3.23
7	10:27	4.8	20.8	46.2	1.97	395.1	20.25	−4.96	232.9	234.5	2.95	−27.83	11.9	4.43
8	12:42	4.9	21.8	37.8	1.93	389.0	20.35	−4.63	239.0	230.1	4.13	−40.50	16.3	6.53
9	15:27	5.3	22.3	37.3	1.93	391.5	20.37	−4.58	240.9	224.7	3.69	−38.73	14.5	5.95
10	17:10	5.7	22.1	37.8	1.95	391.5	20.36	−4.63	208.1	221.2	4.36	−47.20	19.8	7.10
11	19:25	5.8	19.6	52.4	1.93	389.6	20.31	−4.61	193.6	220.4	3.02	−37.17	14.7	5.62
12	20:35	5.2	17.7	61.1	1.95	386.9	20.24	−4.82	158.0	215.8	3.49	−48.11	22.0	7.20

[a]Transect sampling started on August 24 and ended on August 25, 2013.

aluminum caps. Dissolved CH_4 was measured within 1 h in the laboratory by the headspace displacement method[32] on a gas chromatograph equipped with a flame ionization detector (Shimadzu GC 14A); the gas chromatograph was calibrated by injecting at least five different volumes of a 1% methane standard (Supelco, ScottyII analyzed gases, USA).

Weather Station Data. Meteorological parameters, including air temperature, relative humidity, and wind speeds (at 2 m height) as well as vertical profiles of the water temperature and oxygen content were collected by the autonomous weather station LakeESP (Precision Measurement Engineering, USA), located at the deepest point of the lake (69 m). Wind speed data were corrected to 10 m using the simple logarithmic law without atmospheric stability correction.[13,33] See the Supporting Information for sensor specifications.

Turbulent Kinetic Energy (TKE) Dissipation. The pulse-coherent high-resolution acoustic Doppler profiler HR-Aquadopp (Nortek AS, Norway) was moored up looking at 2.2 m beneath the lake surface. The profiler registered three components of the current velocity vector at a sampling rate of 0.5 Hz with a vertical resolution of 0.02 m. The dissipation rate (ε) of TKE was determined using the structure function method and was used later to justify wind speed as proxy for the mixing intensity in the upper water column (see Methods of the Supporting Information).[34]

Gas Flux Calculations and Exchange Velocities. The diffusive flux F ($mol\ m^{-2}\ d^{-1}$) across the air–water interface for an individual gas species i is defined as

$$F_i = k_i(C_{water,i} - H_iP_i) \tag{4}$$

where k ($m\ d^{-1}$) is the transfer velocity (or piston velocity), C_{water} ($mol\ m^{-3}$) is the concentration of the dissolved gas, H ($mol\ m^{-3}\ Pa^{-1}$) is the Henry's coefficient, and P (Pa) is the atmospheric gas partial pressure. As the flux and both the air-side and water-side gas concentrations are measured, the transfer velocity k can be solved by

$$k_i = F_i/(C_{water,i} - H_iP_i) \tag{5}$$

For comparison of transfer velocities between experiments and for different gases, k is adjusted to a Schmidt number (Sc) of 600, where Sc is the ratio of the kinematic viscosity of water to the diffusion coefficient of SF_6 and Sc = 600 is for CO_2 at 20 °C.[13,35] The adjusted k, termed k_{600}, is defined as

$$k_{600} = k_i(600/Sc_i)^{-n} \tag{6}$$

Similar to Guerin et al.[36] and Prairie and del Giorgio,[9] the exponent n is taken as $n = {}^2/_3$ for wind speed < 3.7 m s^{-1} and $n = {}^1/_2$ for wind > 3.7 m s^{-1}.

Microbubble Model. For the microbubble modeling, the discrete-bubble modeling approach was used. The modeling approach here is a simplified, steady-state approach compared to that of Merlivat and Memery.[37] The model predicts the evolution of gases (both dissolution and stripping) across the surface of a single bubble[38,39] as

$$\frac{dM_i}{dt} = K_i(C_{water,i} - H_iP_{bi})A_s \tag{7}$$

where dM_i (mol) is the change of moles in the bubble, t is time (s), K_i (m s^{-1}) is the gas-transfer rate across the bubble surface, A_s (m^2) is the surface area of the bubble, and P_{bi} (Pa) is the gas partial pressure in the bubble. The model was used to estimate the time it takes for a 1 mm diameter air bubble introduced into

the surface layer to become in equilibrium with ambient gases. We used the average dissolved gas concentrations in our study (Table 1) and tracked changes of O_2, CH_4, and CO_2 in the bubble. We assumed dissolved N_2 in the surface water was at atmospheric equilibrium.

For a bubble located at 10 cm depth, the 1 mm diameter bubbles reached equilibrium with ambient dissolved gases in <10 s. As the bubble residence time in the surface layer is likely much longer than 10 s, and as the bubbles are likely smaller than 1 mm,[19] we can therefore assume steady-state to solve for bubble gas partial pressures $P_{bi} = C_{water,i}/H_i$. Henry's coefficients were obtained from Sander.[40] The moles, n, of the particular gas were solved using the ideal gas formulation, $P_{bi}V = nRT$, where V is the volume of the bubble (m^3), T is the temperature (K), and R is the gas constant (8.314 m^3 Pa mol^{-1} K^{-1}).

■ RESULTS

Overview. The onset of penetrative-convective mixing driven by cooling of the lake surface (i.e., lake turnover) had already begun several weeks prior to our study. The surface mixed layer extended down to ~7 m (<0.5 °C change over depth) as indicated by the temperature profiles (Figures S5 and S6 of the Supporting Information). The boat-mounted CH_4 sensor and discrete CH_4 samples from the center of the lake (where the transects were performed) ranged from about 0.5 μmol L^{-1} at the start of the campaign and decreased to about 0.2 μmol L^{-1} toward the end of the campaign (Figure S7 of the Supporting Information; Table 1). The surface mixed layer was oversaturated with O_2 (average ~117% sat), and pCO$_2$ values ranged from about 215 to 240 ppm during the transects (Figure S7 of the Supporting Information). The wind speed varied from about 4 to 6 m s^{-1} and generally increased over time (Figure 1a). The wind speed and dissipation rate of TKE (ε) correlated
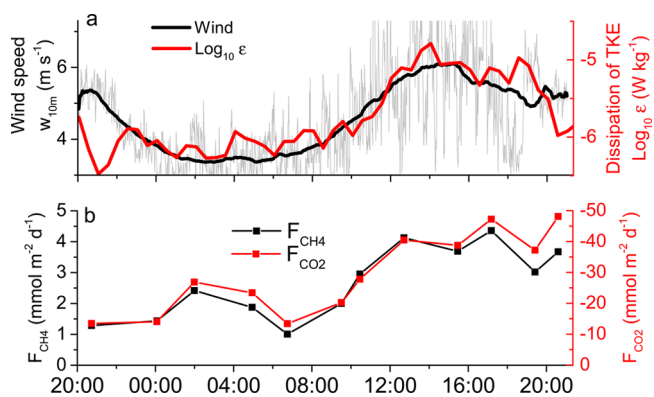

Figure 1. Transect from August 24–25, 2013. (a) Wind speed corrected to 10 m (gray is raw data, black is running mean) and surface turbulence (dissipation rate of TKE measured by AQUA-DOPP) over top 2 m. (b) Time series of CO_2 and CH_4 fluxes (F).

well ($R^2 = 0.94$) excluding the brief period at the beginning of the campaign during transect 1 (August 24 from 20:00 to 22:00; Figure 1a; Figure S8 of the Supporting Information); R^2 was 0.65 including all data. The wind direction was nearly constant and out of the east.

Each of the 12 transects (~200–300 m) over the ~24 h campaign took on average 26 min and was in the direction of the wind (westerly). For each transect, the average of each constituent was calculated (Table 1). The atmospheric CH_4 and CO_2 concentrations were measured with the portable

GHG analyzer at the beginning of each transect. Surface water−air fluxes of CH_4 and CO_2 measured with the floating chamber showed smooth and linear changes of the gas concentrations with time (linear fit correlation $R^2 > 0.98$; Figures S3 and S4 of the Supporting Information), indicating strictly diffusive transport; no abrupt concentration increases associated with sediment-released CH_4 bubbles were observed.[41]

Flux Drivers. The CH_4 and CO_2 fluxes correlated strongly with each other ($R^2 = 0.99$; Figures 1b and 2a), indicating that
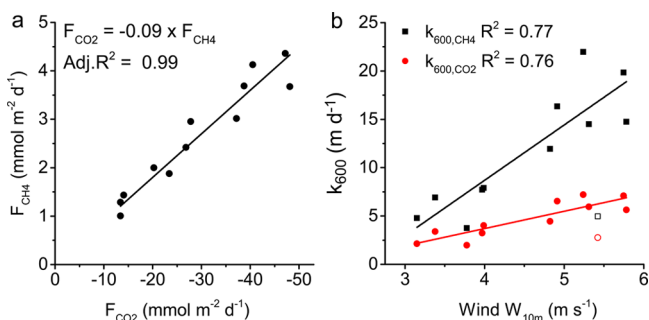

Figure 2. (a) Methane flux vs CO_2 flux indicating an excellent correlation ($R^2 = 0.99$) despite being in opposite directions (CH_4 emission vs CO_2 sink). (b) k_{600} for both gases as a function of wind speed corrected to 10 m. k_{600} correlates well with wind speed, except for first data points (open symbols), which were excluded from the correlation because of the poor relationship between wind and turbulence (see Figure 1).

both were driven by similar processes. The transfer velocities for CO_2, $k_{600,CO2}$, were on average about 2.7 times higher than those calculated on the wind parametrizations after Crusius and Wanninkhof;[13] however, $k_{600,CH4}$ was much (6.7 times) higher (discussed below). The mass-transfer coefficients $k_{600,CH4}$ and $k_{600,CO2}$ correlated well with wind speed (Figure 2b: $R^2 = 0.77$, $R^2 = 0.76$, respectively, note that the first data point is neglected) and the fluxes correlated with turbulence (Figure S9 of the Supporting Information; $R^2 = 0.69$, $R^2 = 0.72$, respectively).

Enhanced $k_{600,CH4}$ and the Role of Microbubbles. While k_{600} values for CH_4 and CO_2 correlated well with one another ($R^2 = 0.96$), $k_{600,CH4}$ was substantially higher. For Fickian transport, k_{600} should be approximately equal for both CH_4 and CO_2 at a given turbulence level. However, we found that $k_{600,CH4}$ was on average ~2.5 times higher than $k_{600,CO2}$ (Figure 3). The difference between $k_{600,CH4}$ and $k_{600,CO2}$ increased with wind speed, to nearly 3 times higher at the maximum wind speed of 5.8 m s^{-1}. This phenomenon has been
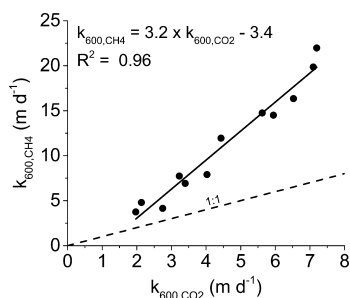

Figure 3. $k_{600,CH4}$ vs $k_{600,CO2}$ with regression (solid line) and the 1:1 line (dashed line).

previously observed in lakes and has been attributed to the presence and exiting of microbubbles from the surface layer.[9] The microbubbles affect CH_4 much more than CO_2 because of CH_4's lower solubility. We explore this hypothesis using a simple bubble model combined with a system-analytical approach.

Microbubble: Analytical Approach. In the following analyses, we assumed the $k_{600,CO2}$ is the baseline Fickian transport for our system and, therefore, can be used to calculate other gas fluxes using eq 4. The purpose was to separate the Fickian flux component from the hypothesized microbubble contribution. In this scenario, microbubbles can either be formed in situ (e.g., O_2 oversaturation from primary production) or be introduced by turbulence due to wave breaking and so forth. For CH_4 and CO_2, either assumption will not affect the outcome. Within the surface layer, the microbubbles strip the sparingly soluble gases (CH_4, N_2, and O_2) from the water into the gas phase and quickly reach equilibrium (see Materials and Methods).

We performed our microbubble analysis in the following steps:

(1) Assume that the $k_{600,CO2}$ is the Fickian gas transfer velocity for all dissolved gases and is thus unaffected by the microbubbles.

(2) Calculate the Fickian CH_4 flux (Figure 4a) using the measured CH_4 concentration driving force ($C_{water,CH4} - H_{CH4}P_{CH4}$) and $k_{600,CO2}$.

(3) Fit a linear regression to both the measured and calculated (Fickian) CH_4 fluxes as a function of wind speed (Figure 4a).

(4) Solve for microbubble CH_4 flux contribution taken as the difference between the two regression lines from step 3 (dashed line, Figure 4a).

(5) Calculate the volume of gas that is necessary to exit the surface layer to produce the microbubble CH_4 flux response (Figure 4b).

(6) Using the gas flux calculated in step 5, we check our assumption in step 1 to see if the CO_2 flux could also potentially be enhanced by the microbubbles (Figure 4b).

(7) Finally, use the microbubble exchange to investigate their effect on O_2 fluxes across the water−air interface.

Microbubble: Analytical Results. On the basis of our analysis, we assume that microbubble contribution to the CH_4 flux (dashed line in Figure 4a) is negligible at winds ≤2 m s^{-1} and reaches a value of ~2.4 mmol m^{-2} d^{-1} at wind speed = 6 m s^{-1}. Using the ideal gas law and the averaged surface dissolved CH_4 concentration, at steady state, a 1 mm diameter bubble in the surface mixed layer would contain ~5.76 × 10^{-9} mmol of CH_4. Using the flux enhancement estimated at a wind speed of 6 m s^{-1} (~2.4 mmol m^{-2} d^{-1}), the expected surface gas exchange would be 0.22 m^3 gas m^{-2} d^{-1} to produce the observed CH_4 flux enhancement.

Role of Microbubbles on CO_2 Flux. The next question is how will this microbubble gas exchange influence the CO_2 flux? In our system, the dissolved pCO_2 was about 50% undersaturated compared to atmospheric concentrations, which is common for Lake Stechlin.[42] Thus, the existing gas bubbles would be similarly undersaturated with respect to atmospheric concentrations, resulting in an apparent CO_2 flux into the water. Each 1 mm diameter bubble at equilibrium would be undersaturated relative to atmospheric equilibrium by ~ −4.2 ×

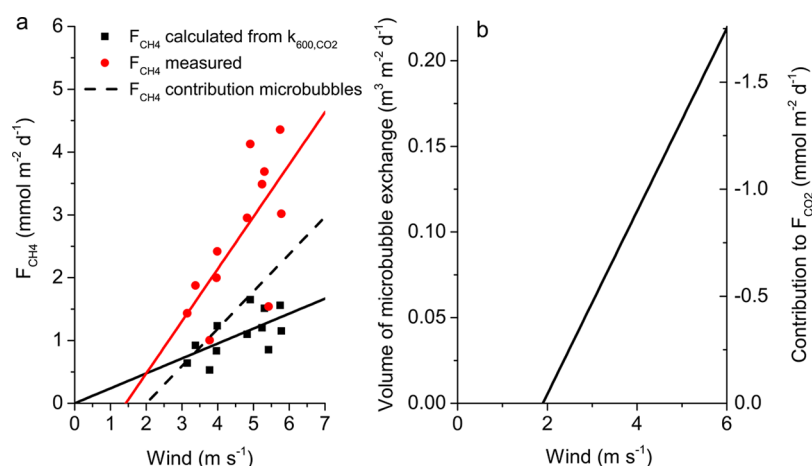**Figure 4.** (a) Measured CH_4 fluxes (red circle) and recalculated CH_4 fluxes using $k_{600,CO2}$ (black square) and their linear fit (solid lines). We take the difference between these as the microbubble flux contribution (dashed black line). (b) Calculated microbubble volume exiting the surface of the lake as a function of wind speed (left axis). Right axis, corresponding microbubble-associated CO_2 flux contribution.

10^{-9} mmol of CO_2. Therefore, for 0.22 m^3 gas m^{-2} d^{-1} (at wind speeds of ~6 m s^{-1}), the flux contribution for CO_2 would only be -1.7 mmol m^{-2} d^{-1} (Figure 4b). This CO_2 flux contribution from the microbubbles accounts for less than 4% of the flux we expect at this wind speed (about -45 mmol m^{-2} d^{-1}), which is not surprising as CO_2 is about 25–30 times more soluble than CH_4.[43]

■ DISCUSSION

Elevated $k_{600,CO2}$. During our campaign, the lake was a CO_2 sink (-1300 mgCO_2 m^{-2} d^{-1}) with elevated CH_4 emissions (43 mg CH_4 m^{-2} d^{-1} or 290 mg C m^{-2} d^{-1} as CO_2 equivalents). Our measured $k_{600,CO2}$ is ~2.7 fold higher than the values estimated according to Crusius and Wanninkhof[13] and are in the same range as those reported by MacIntyre et al.[14] In lakes with high pH and undersaturated CO_2,[44] such as Lake Stechlin,[42] conversion of CO_2 to soluble bicarbonate/ carbonate and their precipitation at high pH (pH in Lake Stechlin >8) can steepen the CO_2 gradient in the diffusive boundary layer and increase k_{600} for CO_2 by 3.5–7.5 times,[45] creating a chemically enhanced diffusion (CED) effect. However, according to Bade and Cole,[45] CED is likely to be significant only in low turbulence situations and would only affect $k_{600,CO2}$ and not $k_{600,CH4}$. Therefore, similar to the conclusions reached by MacIntyre et al.[14] and Eugster et al.,[17] we assume that our k_{600} values are elevated because of associated convective mixing and turbulent processes. This ~2.7 fold increase over the estimates from Crusius and Wanninkhof[13] is therefore a Fickian enhancement and would similarly affect k_{600} for both CO_2 and CH_4.

Microbubble-Elevated $k_{600,CH4}$. Our $k_{600,CH4}$ is on average ~2.5 times higher than $k_{600,CO2}$, slightly higher than the 2.3 fold increase reported by Prairie and del Giorgio.[9] Over our campaign, an average of 145 L m^{-2} d^{-1} of gas must either be exchanged with the atmosphere or be emitted as internally generated microbubbles (or a combination). The microbubble effect on surface mass transfer has long been discussed in marine gas exchange studies[46] but very rarely in freshwaters.[10] To our knowledge, only one publication has suggested microbubbles as an explanation for observed elevated $k_{600,CH4}$.[9]

Origin of Microbubbles in Lake Stechlin. Prairie and del Giorgio[9] suggest that the microbubbles result in supersaturated waters because of seeding by suspended particles or colloids.

Indeed, algal and particle concentrations within the metalimnion of Lake Stechlin, including bacteria, could serve as gas bubble nuclei.[7]

Ramsey[47] studied bubble formation in a marine surface mixed layer in oxygen oversaturated conditions and suggests that for our conditions (O_2 ~ 117% saturation), bubble growth can occur from the surface to a depth of ~65 cm. These free visible bubbles will result because of growth of invisible microbubbles already present in the water column.[47] Being extremely small, these bubbles can have surface layer residence times of up to several days.[23] Additionally, once a free visible bubble is formed, it will have a tendency to rise, and the residence time in the surface mixed layer will decrease. As an example, Melack and Kilham[48] applied the theoretical Ramsey calculations to measured O_2 concentrations in Lake Nakuru (Africa) and calculated that bubbles could theoretically grow at depths of up to 2.5 m over their measurement campaign (see their Figure 3). In fact, the authors were able to collect bubblegas samples with deployed gas traps in the surface layer of the lake to verify the presence of bubbles.

As shown by our data (Figure 4a), microbubble fluxes were related to wind speed and turbulence. Enhanced turbulence could increase the exposure of gas-supersaturated water from deeper in the mixed layer to the near surface, where the bubbles could start growing faster because of lower hydrostatic pressure. Bubble entrainment from the atmosphere is also expected to occur in lakes at wind speeds from 3 to 8 m s^{-1},[17] approximately the same range when we observed our microbubble effects.

In Lake Stechlin and most inland waters, the two gases that can conceivably produce microbubbles in the surface layer are O_2 and N_2. In oxygenated surface water, the partial pressures of these two gases far exceed other background gases, including CH_4, CO_2, and argon (Ar). In the case of Lake Stechlin, besides the supersaturated O_2 during this study, dissolved N_2 concentrations could also be supersaturated. Assuming the lake water reached atmospheric gas equilibrium during spring turnover at ~6 °C, the bottom water concentration of N_2 would be ~730 μM whereas the surface equilibrium concentration at 20 °C would be ~540 μM.[49] As the thermocline was deepening because of penetrative convection, it is conceivable that N_2-rich bottom water upwelled into the warmer surface mixed layer, thus adding to the total dissolved

gas oversaturation, about 131% oversaturation of $N_2 + O_2$, and stimulating the formation of microbubbles.

Implications. The microbubble phenomena can be expected to enhance the flux of all sparingly soluble gases, that is, N_2, O_2, and Ar. For example, using our assumed Fickian k_{600} (for CO_2) together with the measured O_2 concentrations gives an O_2 outgassing of 220 mmol m^{-2} d^{-1} over our transect period. According to our estimates, microbubble enhancement will increase this value to 430 mmol m^{-2} d^{-1}. This will be an important point to consider for estimating carbon balances in the surface productive layers, as O_2 fluxes are often used as proxies for inferring carbon turnover in aquatic systems.[50]

Fall turnover in lakes is an important time for CH_4 outgassing when previously isolated CH_4-rich waters in the hypolimnion and metalimnion are mixed into the surface.[51] However, the relative importance of direct CH_4 emission versus oxidation to CO_2 during the turnover is less clear. For example, Fernandez et al.[52] compared CH_4 emissions and oxidation rates during turnover using a simple mass balance that relied on literature k_{600} values. The authors conclude that only around 50% of the CH_4 reaches the atmosphere, and the remaining is oxidized. However, they also report that using the flux model from MacIntyre et al.[14] increases the released CH_4 proportion to 87% instead of 50%. Our work suggests that their CH_4 emissions to the atmosphere may be even further underestimated if microbubbles were present, a condition which seems likely to have occurred given the high wind speeds measured during their campaign (up to 5−9 m s^{-1}). Therefore, even with a modest 2-fold increase in k_{600} because of microbubbles, the estimated emissions to the atmosphere would approach nearly 100% of the stored CH_4.

Our work demonstrates the potential for considerable CH_4 fluxes and emission from oxic, oligotrophic freshwaters. Using a floating chamber, we directly measured an average CH_4 flux of about 2.6 ± 1.1 mmol m^{-2} d^{-1} (42 mg m^{-2} d^{-1}). These are surprisingly high surface fluxes, especially for an oligotrophic lake. For comparison, these CH_4 fluxes, though only measured over a short period, are a factor of 4.2 times higher than the diffusive fluxes reported for temperate lakes and are over 21 times higher than those in high temperate and subpolar regions.[5] In addition to the microbubble effect, these high CH_4 fluxes are also attributed to the presence of the recently discovered surface-layer methane production in oligotrophic Lake Stechlin.[7,8]

Timing of Fluxes: The Unknown. The effect of wind speed is conspicuous, from no flux enhancement at ≤2 m s^{-1} to ~270% CH_4 flux enhancement at 6 m s^{-1}. The average wind speed of 3.6 m s^{-1} (measured at 2 m height) during the campaign corresponded to 145 L m^{-2} d^{-1} of gas emission via microbubbles. Although multidecadal mean wind speed in Lake Stechlin is below 2 m s^{-1} (1.8 averaged for 1958−2002, see Kirillin et al.[53]), the effect could be significant during periods of sustained gusts. We caution, however, against extrapolating our results in terms of wind speed to other water bodies, as fetch size along with many other factors could affect k_{600}.[16]

Questions remain as to the origin, prevalence, and timing of microbubble formation. Microbubbles could have either originated from (1) atmospheric entrainment of microbubbles, (2) internal production due to gas supersaturation, (3) a combination of both, or (4) some other unknown mechanisms. We speculate that the phenomenon in Lake Stechlin was related to the oncoming penetrative convective mixing (turnover) combined with supersaturated O_2 values, the potential upwelling of N_2-supersaturated water, and wind-generating turbulence or bubble entrainment. The potentially large impact of microbubbles on CH_4 emission from aquatic systems demonstrated here and the subsequent effect on the terrestrial C budgets warrant further investigation.

■ ASSOCIATED CONTENT

ⓢ Supporting Information

Meteorological sensor specifications and the turbulence methods section, nine ancillary figures, including the map of the study site (Figure S1), picture of the floating chamber (Figure S2), and additional figures (Figures S3−S9) demonstrating the background conditions and results. This material is available free of charge via the Internet at http://pubs.acs.org/.

■ AUTHOR INFORMATION

Corresponding Author
*Phone: +41 22 379 0792; e-mail: daniel.mcginnis@unige.ch.

Author Contributions

D. F. McGinnis, S. Flury, K. Tang, G. Kirillin, C. Engelhardt, and H.-P. Grossart conceived, designed, and performed the study. P. Bodmer and S. Flury prepared the sampling equipment (Berlin), and P. Bodmer designed and built the flux chamber. P. Casper and H.-P. Grossart provided equipment and sampling/measurement support from Neuglobsow. D. F. McGinnis, G. Kirilin, and P. Bodmer performed data analysis, and D. F. McGinnis developed and performed the modeling. D. F. McGinnis wrote the manuscript with contributions from all other authors. All authors contributed equally to discussion of the results and manuscript development. All authors have given approval of the final manuscript version.

Notes

The authors declare no competing financial interests.

■ ACKNOWLEDGMENTS

■ REFERENCES

(1) Aufdenkampe, A. K.; Mayorga, E.; Raymond, P. A.; Melack, J. M.; Doney, S. C.; Alin, S. R.; Aalto, R. E.; Yoo, K. Riverine coupling of biogeochemical cycles between land, oceans, and atmosphere. *Front. Ecol. Environ.* **2011**, *9* (1), 53−60.

(2) Battin, T. J.; Luyssaert, S.; Kaplan, L. A.; Aufdenkampe, A. K.; Richter, A.; Tranvik, L. J. The boundless carbon cycle. *Nat. Geosci.* **2009**, *2* (9), 598−600.

(3) Cole, J. J.; Prairie, Y. T.; Caraco, N. F.; McDowell, W. H.; Tranvik, L. J.; Striegl, R. G.; Duarte, C. M.; Kortelainen, P.; Downing, J. A.; Middelburg, J. J.; Melack, J. Plumbing the global carbon cycle: Integrating inland waters into the terrestrial carbon budget. *Ecosystems* **2007**, *10* (1), 171−184.

(4) Tranvik, L. J.; Downing, J. A.; Cotner, J. B.; Loiselle, S. A.; Striegl, R. G.; Ballatore, T. J.; Dillon, P.; Finlay, K.; Fortino, K.; Knoll, L. B.; Kortelainen, P. L.; Kutser, T.; Larsen, S.; Laurion, I.; Leech, D. M.; McCallister, S. L.; McKnight, D. M.; Melack, J. M.; Overholt, E.; Porter, J. A.; Prairie, Y.; Renwick, W. H.; Roland, F.; Sherman, B. S.; Schindler, D. W.; Sobek, S.; Tremblay, A.; Vanni, M. J.; Verschoor, A. M.; von Wachenfeldt, E.; Weyhenmeyer, G. A. Lakes and reservoirs as regulators of carbon cycling and climate. *Limnol. Oceanogr.* **2009**, *54* (6), 2298−2314.

(5) Bastviken, D.; Tranvik, L. J.; Downing, J. A.; Crill, P. M.; Enrich-Prast, A. Freshwater methane emissions offset the continental carbon sink. *Science* **2011**, *331* (6013).

(6) Forster, P.; Ramaswamy, V.; Artaxo, P.; Berntsen, T.; Betts, R.; Fahey, D. W.; Haywood, J.; Lean, J.; Lowe, D. C.; Myhre, G.; Nganga, J.; Prinn, R.; Raga, G.; Schulz, M.; Van Dorland, R. *Changes in Atmospheric Constituents and in Radiative Forcing*; In: Climate Change 2007: The Physical Science Basis. Contribution of Working Group I to the Fourth Assessment Report of the Intergovernmental Panel on Climate Change; Solomon, S., Qin, D., Manning, M., Chen, Z., Marquis, M., Averyt, K. B., Tignor, M., Miller, H.L., Eds.; Cambridge University Press: Cambridge, United Kingdom and New York, NY, USA, 2007.

(7) Grossart, H.-P.; Frindte, K.; Dziallas, C.; Eckert, W.; Tang, K. W. Microbial methane production in oxygenated water column of an oligotrophic lake. *Proc. Natl. Acad. Sci. U.S.A.* **2011**, *108* (49), 19657−19661.

(8) Tang, K. W.; McGinnis, D. F.; Frindte, K.; Bruchert, V.; Grossart, H. P. Paradox reconsidered: Methane oversaturation in well-oxygenated lake waters. *Limnol. Oceanogr.* **2014**, *59* (1), 275−284.

(9) Prairie, Y. T.; del Giorgio, P. A. A new pathway of freshwater methane emissions and the putative importance of microbubbles. *Inland Waters* **2013**, *3* (3), 311−320.

(10) Beaulieu, J. J.; Shuster, W. D.; Rebholz, J. A. Controls on gas transfer velocities in a large river. *J. Geophys. Res.: Biogeosci.* **2012**, *117*.

(11) Cole, J. J.; Bade, D. L.; Bastviken, D.; Pace, M. L.; Van de Bogert, M. Multiple approaches to estimating air-water gas exchange in small lakes. *Limnol. Oceanogr. Meth.* **2010**, *8*, 285−293.

(12) Jahne, B.; Munnich, K. O.; Bosinger, R.; Dutzi, A.; Huber, W.; Libner, P. On the parameters influencing air-water gas-exchange. *J. Geophys. Res.: Oceans* **1987**, *92* (C2), 1937−1949.

(13) Crusius, J.; Wanninkhof, R. Gas transfer velocities measured at low wind speed over a lake. *Limnol. Oceanogr.* **2003**, *48* (3), 1010−1017.

(14) MacIntyre, S.; Jonsson, A.; Jansson, M.; Aberg, J.; Turney, D. E.; Miller, S. D. Buoyancy flux, turbulence, and the gas transfer coefficient in a stratified lake. *Geophys. Res. Lett.* **2010**, *37*.

(15) Heiskanen, J. J.; Mammarella, I.; Haapanala, S.; Pumpanen, J.; Vesala, T.; Macintyre, S.; Ojala, A. Effects of cooling and internal wave motions on gas transfer coefficients in a boreal lake. *Tellus, Ser. B: Chem. Phys. Meteorol.* **2014**, *66*.

(16) Vachon, D.; Prairie, Y. T.; Cole, J. J. The relationship between near-surface turbulence and gas transfer velocity in freshwater systems and its implications for floating chamber measurements of gas exchange. *Limnol. Oceanogr.* **2010**, *55* (4), 1723−1732.

(17) Eugster, W.; Kling, G.; Jonas, T.; McFadden, J. P.; Wüest, A.; MacIntyre, S.; Chapin, F. S. CO2 exchange between air and water in an Arctic Alaskan and midlatitude Swiss lake: Importance of convective mixing. *J. Geophys. Res.: Atmos.* **2003**, *108* (D12).

(18) Cole, J. J.; Caraco, N. F. Atmospheric exchange of carbon dioxide in a low-wind oligotrophic lake measured by the addition of SF6. *Limnol. Oceanogr.* **1998**, *43* (4), 647−656.

(19) Wu, J. Bubble populations and spectra in near-surface ocean - summary and review of field-measurements. *J. Geophys. Res.: Oceans Atmos.* **1981**, *86* (NC1), 457−463.

(20) Kanwisher, J. On the exchange of gases between the atmosphere and the sea. *Deep−Sea Res.* **1963**, *10* (3), 195 ff.

(21) Vagle, S.; McNeil, C.; Steiner, N. Upper ocean bubble measurements from the NE Pacific and estimates of their role in air-sea gas transfer of the weakly soluble gases nitrogen and oxygen. *J. Geophys. Res.: Oceans* **2010**, *115*.

(22) Thorpe, S. A.; Osborn, T. R.; Farmer, D. M.; Vagle, S. Bubble clouds and Langmuir circulation: Observations and models. *J. Phys. Oceanogr.* **2003**, *33* (9), 2013−2031.

(23) Turner, W. R. Microbubble persistence in fresh water. *J. Acoust. Soc. Am.* **1961**, *33* (9), 1223 ff.

(24) *Lake Stechlin: A Temperate Oligotrophic Lake*; Casper, J. S., Ed.; Kluwer Academic Publishers: Dordrecht, Boston, 1985.

(25) Koschel, R.; Adams, D. D. *Lake Stechlin - An approach to understanding a temperate oligotrophic lowland lake*; Schweizerbart Science Publishers: Stuttgart, Germany, 2003; Vol. 58.

(26) Casper, P.; Adams, D. D.; Furtado, A. L. S.; Chan, O. C.; Gonsiorczyk, T.; Koschel, R. Greenhouse gas cycling in aquatic ecosystems − Methane in temperate lakes across an environmental gradient in NE Germany. *Verh. Int. Ver. Limnol.* **2005**, *29*, 564−566.

(27) Casper, P.; Furtado, A. L. S.; Adams, D. D. Biogeochemistry and diffuse fluxes of greenhouse gases (methane and carbon dioxide) and dinitrogen from the sediments of oligotrophic Lake Stechlin, Northern Germany. *Arch. Hydrobiol. Spec. Issues Adv. Limnol.* **2003**, *58*, 53−71.

(28) Conrad, R.; Chan, O.-C.; Claus, P.; Casper, P. Characterization of methanogenic Archaea and stable isotope fractionation during methane production in the profundal sediment of an oligotrophic lake (Lake Stechlin, Germany). *Limnol. Oceanogr.* **2007**, *52* (4), 1393−1406.

(29) Casper, P. Methane production in littoral and profundal sediments of an oligotrophic and a eutrophic lake. *Arch. Hydrobiol. Spec. Issues Adv. Limnol.* **1996**, *48*, 253−259.

(30) Galfalk, M.; Bastviken, D.; Fredriksson, S.; Arneborg, L. Determination of the piston velocity for water-air interfaces using flux chambers, acoustic Doppler velocimetry, and IR imaging of the water surface. *J. Geophys. Res.: Biogeosci.* **2013**, *118* (2), 770−782.

(31) Fietzek, P.; Fiedler, B.; Steinhoff, T.; Koertzinger, A. In situ quality assessment of a novel underwater pCO(2) sensor based on membrane equilibration and NDIR spectrometry. *J. Atmos. Ocean. Technol.* **2014**, *31* (1), 181−196.

(32) Schmidt, U.; Conrad, R. Hydrogen, carbon-monoxide, and methane dynamics in Lake Constance. *Limnol. Oceanogr.* **1993**, *38* (6), 1214−1226.

(33) Donelan, M. *Air-sea interaction, the sea: Ocean engineering science*; Wiley: New York, 1990.

(34) Wiles, P. J.; Rippeth, T. P.; Simpson, J. H.; Hendricks, P. J. A novel technique for measuring the rate of turbulent dissipation in the marine environment. *Geophys. Res. Lett.* **2006**, *33* (21), L21608.

(35) Wanninkhof, R. Relationship between wind speed and gas exchange over the ocean. *J. Geophys. Res.* **1992**, *97*, 7373−7382.

(36) Guerin, F.; Abril, G.; Serca, D.; Delon, C.; Richard, S.; Delmas, R.; Tremblay, A.; Varfalvy, L. Gas transfer velocities of CO2 and CH4 in a tropical reservoir and its river downstream. *J. Mar. Syst.* **2007**, *66* (1−4), 161−172.

(37) Merlivat, L.; Memery, L. Gas-exchange across an air-water-interface - experimental results and modeling of bubble contribution to transfer. *J. Geophys. Res.: Oceans Atmos.* **1983**, *88* (NC1), 707−724.

(38) McGinnis, D. F.; Greinert, J.; Artemov, Y.; Beaubien, S. E.; Wüest, A. Fate of rising methane bubbles in stratified waters: How much methane reaches the atmosphere? *J. Geophys. Res.: Oceans* **2006**, *111* (C9), 15.

(39) McGinnis, D. F.; Little, J. C. Predicting diffused-bubble oxygen transfer rate using the discrete-bubble model. *Water Res.* **2002**, *36* (18), 4627−4635.

(40) Sander, R. Compilation of Henry's Law constants for inorganic and organic species of potential importance in environmental

chemistry (Version 3). http://www.henrys-law.org (accessed June 17, 2014.

(41) Nguyen Thanh, D.; Silverstein, S.; Lundmark, L.; Reyier, H.; Crill, P.; Bastviken, D. Automated flux chamber for investigating gas flux at water-air interfaces. *Environ. Sci. Technol.* **2013**, *47* (2), 968−975.

(42) Gelbrecht, J.; Fait, M.; Dittrich, M.; Steinberg, C. Use of GC and equilibrium calculations of CO2 saturation index to indicate whether freshwater bodies in north-eastern Germany are net sources or sinks for atmospheric CO2. *Fresenius' J. Anal. Chem.* **1998**, *361* (1), 47−53.

(43) McGinnis, D. F.; Schmidt, M.; DelSontro, T.; Themann, S.; Rovelli, L.; Reitz, A.; Linke, P. Discovery of a natural CO2 seep in the German North Sea: Implications for shallow dissolved gas and seep detection. *J. Geophys. Res.: Oceans* **2011**, *116*, 12.

(44) Wanninkhof, R.; Knox, M. Chemical enhancement of CO2 exchange in natural waters. *Limnol. Oceanogr.* **1996**, *41* (4), 689−697.

(45) Bade, D. L.; Cole, J. J. Impact of chemically enhanced diffusion on dissolved inorganic carbon stable isotopes in a fertilized lake. *J. Geophys. Res.: Oceans* **2006**, *111* (C1).

(46) Woolf, D. K.; Leifer, I. S.; Nightingale, P. D.; Rhee, T. S.; Bowyer, P.; Caulliez, G.; de Leeuw, G.; Larsen, S. E.; Liddicoat, M.; Baker, J.; Andreae, M. O. Modelling of bubble-mediated gas transfer: Fundamental principles and a laboratory test. *J. Mar. Syst.* **2007**, *66* (1−4), 71−91.

(47) Ramsey, W. L. Bubble growth from dissolved oxygen near the sea surface. *Limnol. Oceanogr.* **1962**, *7* (1), 1−7.

(48) Melack, J. M.; Kilham, P. Photosynthetic rates of phytoplankton in east-african alkaline, saline lakes. *Limnol. Oceanogr.* **1974**, *19* (5), 743−755.

(49) Wüest, A.; Brooks, N. H.; Imboden, D. M. Bubble plume modeling for lake restoration. *Water Resour. Res.* **1992**, *28* (12), 3235−3250.

(50) Glud, R. N. Oxygen dynamics of marine sediments. *Mar. Biol. Res.* **2008**, *4* (4), 243−289.

(51) Schubert, C. J.; Diem, T.; Eugster, W. Methane emissions from a small wind shielded lake determined by eddy covariance, flux chambers, anchored funnels, and boundary model calculations: a comparison. *Environ. Sci. Technol.* **2012**, *46* (8), 4515−4522.

(52) Fernandez, J. E.; Peeters, F.; Hofmann, H. Importance of the autumn overturn and anoxic conditions in the hypolimnion for the annual methane emissions from a temperate lake. *Environ. Sci. Technol.* **2014**, *48*, 7297 −7304.

(53) Kirillin, G.; Phillip, W.; Engelhardt, C.; Nuetzmann, G. Net groundwater inflow in an enclosed lake: from synoptic variations to climatic projections. *Hydrol. Processes* **2013**, *27* (3), 347−359.